Conference materials
UDC 539.412.1
DOI: https://doi.org/10.18721/JPM.161.230

Nanostructured high-strength high-modulus film polymer materials: statistical elastic and fracture mechanical properties

Yu.M. Boiko✉, V.A. Marikhin, L.P. Myasnikova

Ioffe Institute, St. Petersburg, Russia

✉ yuri.boiko@mail.ioffe.ru

Abstract. The statistical distributions of the mechanical properties (strength σ, strain at break ε_b, and Young's modulus E) of the high-strength high-modulus oriented thin films and fibers of polyamide-6 (PA-6) have been investigated. For this purpose, two types of the PA-6 samples have been selected: single thin threads and multifilament fibers consisting of some hundreds of individual fibers. The statistical analysis has been carried out on a large number of mechanical tests of identical samples (50 testing samples for each of the two sample types) using the Gaussian and Weibull's models. Beside the 'traditional' mechanical properties (σ, ε_b, and E) commonly used for materials characterization, two additional viscoelastic and fracture characteristics have been estimated and introduced when analyzing the stress-strain curve by taking its first derivative. These are the tangent to the linear viscoelastic portion of the stress-strain curve at relatively large strains (6–14%) and the deformation interval between ε_b and the strain value received by extrapolation of this curve portion to σ = 0, referred to as the apparent viscoelastic modulus (E_2) and apparent strain at break (ε_{b-2}), respectively. The similarities and differences of the statistical distribution behaviors of σ, ε_b, E, E_2, and ε_{b-2} for two PA-6 sample types investigated, including the applicability of the Gaussian and Weibull's models, have been discussed.

Keywords: polyamide-6, fibers, mechanical properties, statistics

Funding: This study was carried out in the framework of the State Task "Strength Physics Problems: Processes of Fracture of Solids, Principles of Materials Strengthening and Enhancement of Materials Dynamical Strength, Development of Crack- and Wear-Resistant Materials" (theme number 0040-2014-0008).

Citation: Boiko Yu.M., Marikhin V.A., Myasnikova L.P., Nanostructured high-strength high-modulus film polymer materials: statistical elastic and fracture mechanical properties, St. Petersburg State Polytechnical University Journal. Physics and Mathematics. 16 (1.2) 2023 196–203. DOI: https://doi.org/10.18721/JPM.161.230

Материалы конференции
УДК 539.412.1
DOI: https://doi.org/10.18721/JPM.161.230

Наноструктурированные высокопрочные высокомодульные пленочные полимерные материалы: статистические упругие и прочностные механические свойства

Ю.М. Бойко✉, В.А. Марихин, Л.П. Мясникова

Физико-технический институт им. А.Ф. Иоффе РАН, Санкт-Петербург, Россия

✉ yuri.boiko@mail.ioffe.ru

Аннотация. Исследованы статистические механические свойства высокопрочных высокомодульных ориентированных тонких пленок и волокон полиамида6-. Обсуждается применимость статистических моделей Гаусса и Вейбулла для описания распределений ряда упругих и прочностных характеристик.

Ключевые слова: полиамид-6, волокна, механические свойства, статистика

Финансирование: Работа выполнена в рамках Государственного задания «Проблемы физики прочности: процессы разрушения твердых тел, принципы упрочнения материалов и повышения динамической прочности материалов, создание трещиностойких, износостойких материалов» (код темы [0008-2014-0040]).

Ссылка при цитировании: Бойко Ю.М., Марихин В.А., Мясникова Л.П. Наноструктурированные высокопрочные высомодульные пленочные полимерные материалы: статистические упругие и прочностные механические свойства // Научно-технические ведомости СПбГПУ. Физико-математические науки. 2023. Т. 1.2 № .16. С. 196–203. DOI: https://doi.org/10.18721/JPM.161.230

Introduction

As is known [1], the orientational drawing behavior of isotropic low-strength polymers is an effective way for producing high-strength high-modulus oriented polymer thin films and multifilament fibers which are the perspective materials in various fields of application. It has been shown that, in the course of orientation, the initial lamellar nanostructure (stacks of folded crystalline lamellae) is transformed into a fibrillar structure (oriented nanofibrils) due to the unfolding of polymer chain folds in the initial lamellae. Such a discrete nanostructural improvement of the material leads to a significant (by an order of magnitude or more) increase in the important mechanical characteristics of the material: Young's (or elastic) modulus (E) up to 200 GPa and strength (σ) up to 6 GPa [1, 2]. However, a negative consequence of this process is the embrittlement of the material, which leads to a sharp increase in the scatter of the measurement results. This behavior is due to the appearance and development of surface nanocracks at the final stages of orientational drawing, the so-called kink bands, which are the initiators of the growth of the main crack during sample failure.

The materials mechanical properties of a common use such as σ, E, and strain at break (ε_b) are important characteristics playing a key role in choosing the most appropriate fields of materials applications. It is generally believed that five tests of identical samples are sufficient to characterize the material by estimating the mean (average) value of σ, ε_b, or E (σ_{av}, ε_{av}, or E_{av}) [3, 4]. However, in some cases, for high-strength high-modulus oriented polymer materials which are quasi-brittle, the scatter of the measured values of mechanical properties is rather broad. Hence, the test number should be increased markedly, up to some tens or even hundreds, in order to estimate correctly the values of σ_{av}, ε_{av}, or E_{av} [2, 5–9]. This makes it possible not only to estimate the values of σ_{av}, ε_{av} and E_{av} more reliably, but to perform the statistical analysis of the distributions of mechanical properties. Information received from such an analysis, for instance, the conformity to a certain theoretical model (e.g., Gaussian, Weibull's [5–11]), can be helpful for a better understanding of the deformation and fracture mechanisms of materials and making a more proper recommendation on their practical use. Actually, if the *distribution* of a measured *data* set can be represented with a bell curve that is characteristic of the *Gaussian* (*or normal) distribution,* it implies that the data *scatter* is caused by the sum of many independent and equally weighted factors [3, 5]. By contrast, if it obeys the Weibull's statistics, it should have the shape of a linear plot in specific coordinates $\ln\ln[1/(1 - P_j)] - \ln\sigma$, where P_j is the cumulative probability of failure, that is indicative of the dominant role in the sample fracture of the surface cracks and their propagation across the sample cross-section [6–11].

Weibull's statistics, proposed initially for σ only, is based on the idea that the fracture of the whole sample is controlled by weakest (local) link [6]. In this approach, the cumulative probability function $P(\sigma)$ describing the probability of failure of identical samples at or below stress σ is given by

$$P(\sigma) = 1 - \exp\left[-(\sigma/\sigma_0)^m\right], \tag{1}$$

where m is the so-called Weibull modulus (a measure of data dispersion) and σ_0 is the scale parameter (having the physical meaning of σ_{av}).

For carrying out Weibull's analysis, a set of test results should be converted into an experimental probability distribution by ordering them from the lowest strength to highest ones. The jth result in the set of n samples is assigned a cumulative probability of failure (P_j)

$$P_j = (j - 0.5)/n. \tag{2}$$

By rearranging Eq. (1), taking logarithm of its both sides twice and replacing $P(\sigma)$ with P_j, Eq. (3) is obtained

$$\ln\ln[1/(1 - P_j)] = -m\cdot\ln\sigma_0 + m\cdot\ln\sigma. \tag{3}$$

In fact, Eq. (3) represents a linear regression

$$y = a + bx, \tag{4}$$

where $y = \ln\ln[1/(1 - P_j)]$, b is the m, x is the $\ln\sigma$, and $a = -m\cdot\ln\sigma_0$ is the curve intersect with the y axis. By estimating m as the tangent to the curve $\ln\ln[1/(1 - P_j)] = f(\ln\sigma)$ using a standard procedure of the linear regression analysis, we can calculate σ_0 by solving Eqs. (5) and (6):

$$\ln\sigma_0 = -a/m, \tag{5}$$

$$\sigma_0 = \exp(-a/m). \tag{6}$$

Earlier [12], it has been suggested to apply this approach, along with σ, to ε_b and E as well. So, by replacing the values of σ and σ_0 in Eqs. (1) and (3) by ε_b and ε_0, and E and E_0, we obtain:

$$\ln\ln[1/(1 - P_j)] = m\cdot\ln\varepsilon_b - m\cdot\ln\varepsilon_0, \tag{7}$$

$$\varepsilon_0 = \exp(-a/m), \tag{8}$$

$$\ln\ln[1/(1 - P_j)] = m\cdot\ln E - m\cdot\ln E_0, \tag{9}$$

$$E_0 = \exp(-a/m). \tag{10}$$

Eqs. (7) and (9) can be reduced to Eq. (4), by analogy with σ, where $x = \ln\varepsilon_b$ or $\ln E$, and $a = -m\cdot\ln\varepsilon_0$ or $a = -m\cdot\ln E_0$.

In order to analyze the stress-strain behavior of high-strength oriented polymers in more detail than traditionally (to analyze σ, ε_b, and E only), the first derivative of the stress-strain curves should be calculated and specific points found (see [12]). In this work, for the first time, the statistical analysis of other mechanical properties found on the stress-strain curves will be performed for the high-strength fibers of polyamide-6 (PA-6) of two types: single and multifilament fibers. The choice of these two different sample types was motivated by their different statistical natures: 'statistical' multifilament sample (consisting of two hundreds of individual fibers) and 'non-statistical' single fiber.

Materials and Methods

The commercial PA-6 single filament with a diameter d of 0.20 mm and the PA-6 multifilament consisting of ~200 individual fibers with a linear density of 213 tex, i.e., with an effective sample d = 0.52 mm or individual fiber d = 2.6 μm, have been used. The force-displacement curves were recorded on an *Instron*-1122 tensile tester at ambient temperature at a cross-head speed of 200 mm/min and a distance between the clamps of 500 mm, i.e., at a strain rate of 0.4 min^{-1}. In order to receive statistically correct results, 50 identical samples were tested for each of the sample types.

Results and Discussion

Fig. 1,*a* shows the stress-strain curves for the oriented mono- and multifilament PA-6 fibers. For the two sample types, the slopes of the curves become steeper at ε >6%, indicating that some strengthening takes place. This behavior suggests that the potential of strengthening has not been realized in the course of drawing and its conditions were not optimal. To put it differently, even after drawing the samples by 10% only, the mechanical properties can be enhanced markedly. Let us consider the stress-strain curves in more detail by differentiating them (see Fig. 1,*b*). As is seen, there are two linear curve portions characterizing with the Young's modulus E_1 at small strains < 1% and an apparent modulus E_2 at large strains >5%. By extrapolating the second curve portion E_2 to $\sigma = 0$, the value of strain at break $\varepsilon_{b\text{-}2}$ for this range of ε can be estimated.

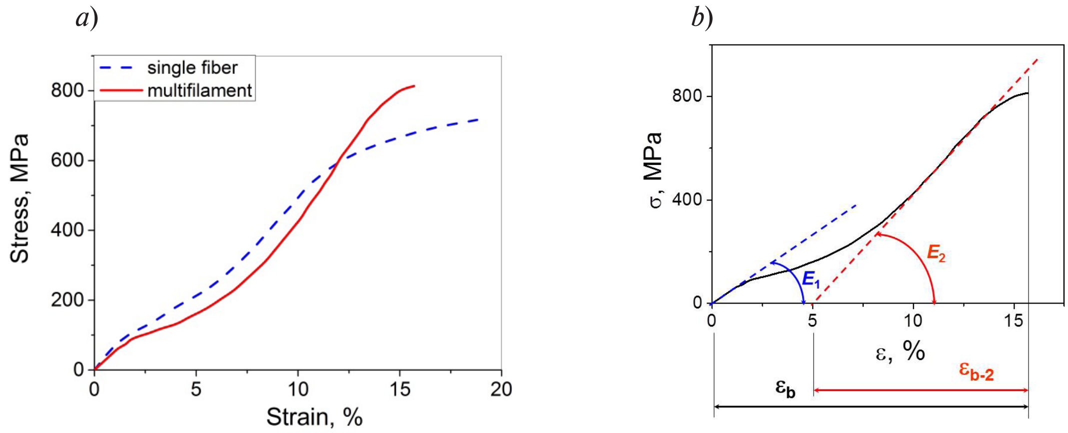

Fig. 1. Stress vs engineering strain for oriented mono- and multifilament PA-6 fibers (*a*), and the scheme of the analysis of the stress-strain curve for the multifilament PA-6 fibers (*b*)

Let us apply the Weibull's and Gaussian models to describe the statistical distributions of the values of E_2 and $\varepsilon_{b\text{-}2}$ presented in Figs. 2,*a* and 3,*a*, respectively. For this purpose, the values of ε_b, ε_0, E, and E_0 in Eqs. (7–10) can be replaced by the corresponding values of $\varepsilon_{b\text{-}2}$, $\varepsilon_{2\text{-}0}$, E_2, and $E_{2\text{-}0}$. As a result, one obtains Eqs. (11–14) that will be used for the Weibull's analysis of E_2 and $\varepsilon_{b\text{-}2}$.

$$\ln\ln[1/(1 - P_j)] = m\cdot\ln\varepsilon_{b\text{-}2} - m\cdot\ln\varepsilon_{2\text{-}0}, \tag{11}$$

$$\varepsilon_{2\text{-}0} = \exp(-a/m), \tag{12}$$

$$\ln\ln[1/(1 - P_j)] = m\cdot\ln E_2 - m\cdot\ln E_{2\text{-}0}, \tag{13}$$

$$\ln E_{2\text{-}0} = \exp(-a/m). \tag{14}$$

The results of the Weibull's analysis of the distributions of E_2 and $\varepsilon_{b\text{-}2}$ are shown in Fig. 2,*b* and 3,*b*, respectively. By analogy, the statistical distributions of the values of σ, ε_b, and $\mathbf{E}_1$ have been analyzed. The results of this analysis for the five mechanical properties (p) under investigation (σ, ε_b, E_1, $\varepsilon_{b\text{-}2}$, and E_2) are collected in Table 1.

As is seen, all the values of the ratio of the scale parameter to the average value p_0/p_{av} ($E_{2\text{-}0}/E_{2\text{-av}}$, $\varepsilon_{2\text{-}0}/\varepsilon_{2\text{-av}}$, $E_{1\text{-}0}/E_{av}$, σ/σ_{av}, and $\varepsilon_0/\varepsilon_{av}$) presented in Table 1 for the two sample types investigated are close to 1 ($p_0/p_{av} \approx 1$), indicating that the Weibull analysis carried out is correct for all the five mechanical properties investigated. For estimating the effect of the deformation strengthening at the second portion of the stress-strain curve, let us compare statistically correct values of E_1 and E_2, i.e., the values of $E_{1\text{-}0}$ and $E_{2\text{-}0}$, respectively, calculated from the corresponding Weibull's plots. Since the ratio $E_{2\text{-}0}/E_{1\text{-}0}$ for the single and multifilament PA-6 fibers are 0.98 and 1.55, respectively, it means that the slope of the second portion ($\varepsilon > 6\%$) of the stress-strain curve for the PA-6 multifilament is steeper with respect to its initial portion ($\varepsilon < 1\%$) while those for the single fibers are equal. This suggests a marked effectiveness of strengthening of the PA-6 multifilament. It should also be noted that the applicability of the Weibull's model is more correct for a fracture property ($\varepsilon_{b\text{-}2}$, $R^2 > 0.96$) with respect to a viscoelastic property (E_2, $R^2 < 0.94$). This behavior seems to be reasonable since this model has been proposed initially namely for a fracture property (σ). The values of m for the two sample types investigated are compared in Table 2. It is seen that they are rather close for E_1 and σ while they are markedly larger for the multifilament, by a factor of 3 to 4, for E_2, ε_b, and $\varepsilon_{b\text{-}2}$. It means that the data scatter for the multifilament is substantially smaller with respect to that for the single fiber. This behavior may be explained by an extremely large number of the fractured single fibers per one test for the multifilament sample including 200 single fibers with respect to the monofilament sample (200 against 1), making the results for the former more proper statistically.

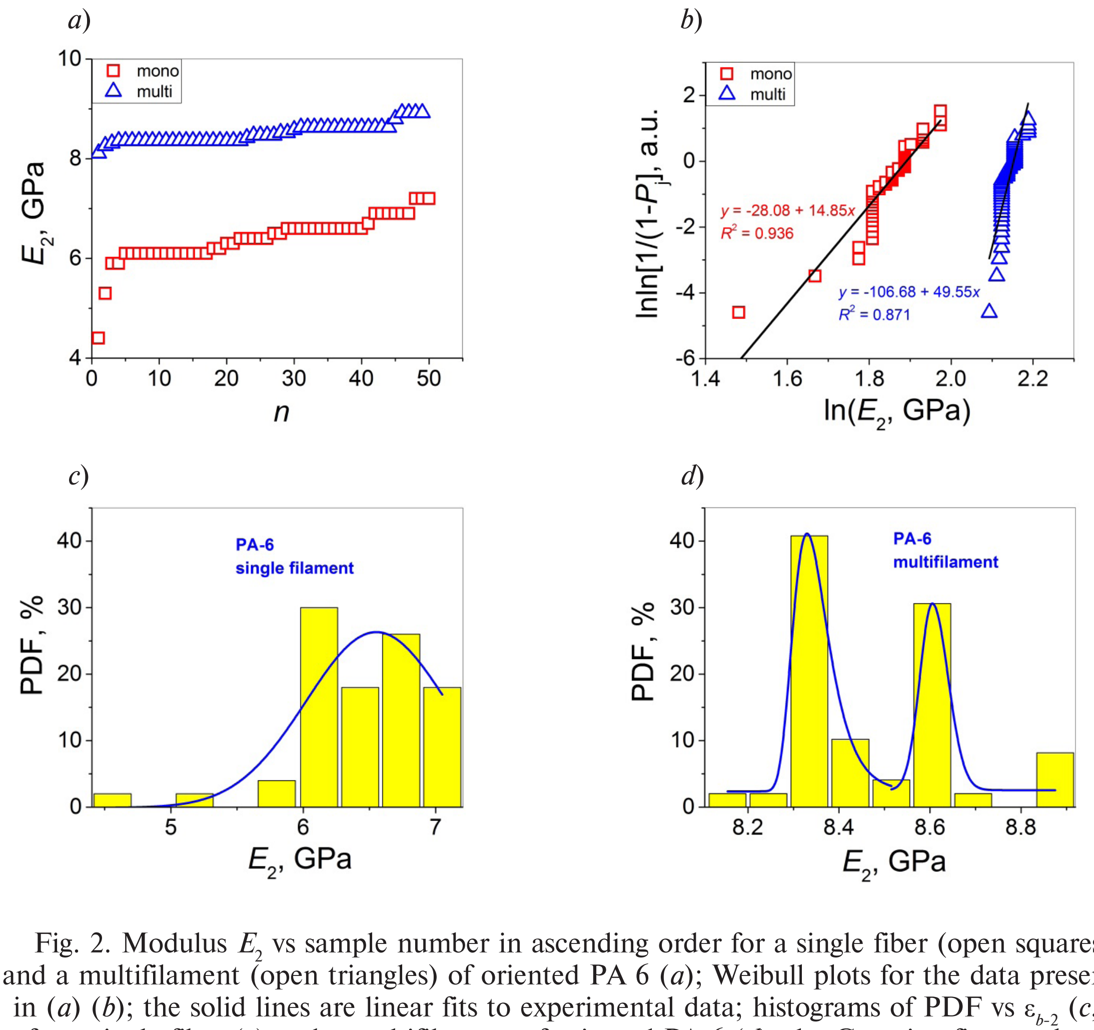

Fig. 2. Modulus E_2 vs sample number in ascending order for a single fiber (open squares) and a multifilament (open triangles) of oriented PA 6 (*a*); Weibull plots for the data presented in (*a*) (*b*); the solid lines are linear fits to experimental data; histograms of PDF vs $\varepsilon_{b\text{-}2}$ (*c*, *d*) for a single fiber (*c*) and a multifilament of oriented PA 6 (*d*); the Gaussian fits are shown with bell-shaped solid curves

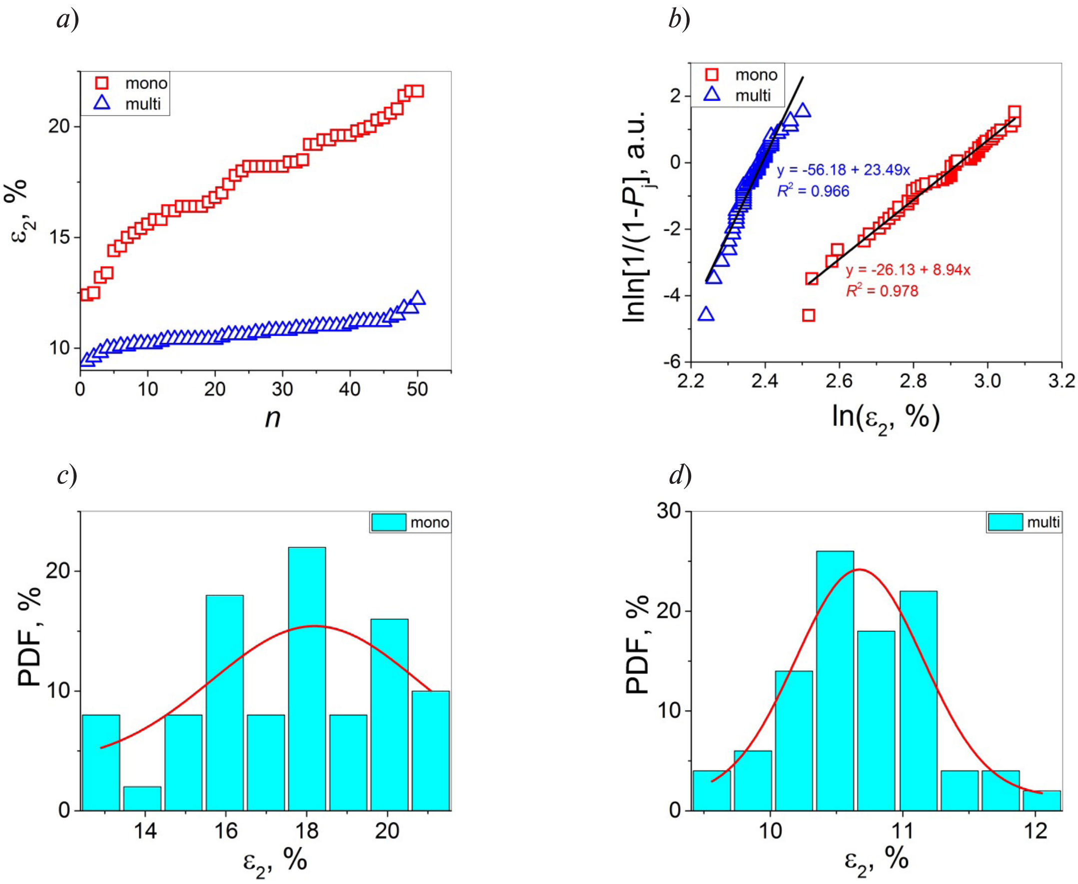

Fig. 3. Extrapolated strain at break $\varepsilon_{b\text{-}2}$ vs sample number in ascending order for a single fiber (open squares) and a multifilament fiber (open triangles) of oriented PA 6 (*a*); its Weibull plots; the solid lines are linear fits to experimental data (*b*); histograms of PDF vs $\varepsilon_{b\text{-}2}$ for a single fiber (*c*) and a multifilament of oriented PA 6 (*d*); the Gaussian fits are shown with bell-shaped solid curves

Table 1

Results of the Weibull analysis of the distributions of various mechanical properties of high-strength single and multifilament fibers of PA-6

Sample type	Property, p	$y = a + bx$	R^2	m	p_0	p_{av}	p_0/p_{av}
single	E_2	$y = -28.08 + 14.85x$	0.936	14.85	6.63 GPa	6.40 GPa	1.04
multi		$y = -106.68 + 49.55x$	0.871	49.55	8.62 GPa	8.56 GPa	1.01
single	$\varepsilon_{b\text{-}2}$	$y = -26.13 + 8.94x$	0.978	8.94	18.6%	17.6%	1.06
multi		$y = -56.18 + 23.49x$	0.966	23.49	10.9%	10.7%	1.02
single	E_1	$y = -44.63 + 23.39x$	0.907	23.39	6.75 GPa	6.60 GPa	1.02
multi		$y = -29.55 + 17.24x$	0.940	17.24	5.56 GPa	5.38 GPa	1.03
single	σ	$y = -297.94 + 45.32x$	0.936	45.32	0.72 GPa	0.71 GPa	1.02
multi		$y = -291.42 + 43.41x$	0.982	43.41	0.83 GPa	0.81 GPa	1.02
single	ε_b	$y = -28.48 + 9.40x$	0.982	9.40	20.7%	19.6%	1.06
multi		$y = -97.06 + 35.01x$	0.958	35.01	16.0%	16.1%	0.99

Table 2

Ratios of *m* for multi- to monofilament PA-6 fibers for a number of mechanical properties

Mechanical property	E_1	σ	ε_b	E_2	$\varepsilon_{b\text{-}2}$
m(multi)/*m*(single)	0.74	0.96	3.72	3.34	2.63

As far as the Gaussian analysis is concerned, the results received turned out to be of various degree of success. Actually, only one (see Fig. 3,*d*, $\varepsilon_{b\text{-}2}$ for multifilament) of the four histograms presented in Figs. 2, *c*, *d* and 3, *c*, *d* can be considered as a bell curve that is characteristic of the normal (Gaussian) distribution. Concerning the distribution of the E_2 values, a bell curve is observed for the single fibers (see Fig. 2,*c*). However, it has an asymmetric shape. Moreover, for the multifilament fibers (see Fig. 2,*d*), a set of the E_2 values demonstrates bimodal distribution. These two observations indicate that the applicability of the Gaussian model for describing the statistical distributions of E_2 and $\varepsilon_{b\text{-}2}$ is rather limited, suggesting that the distributions of E_2 and $\varepsilon_{b\text{-}2}$ is not always controlled by the sum of many independent and equally weighted factors.

Conclusion

The marked effect of strengthening of the PA-6 multifilament in the course of tensile testing has been found, indicating that the enhancement of the mechanical properties proceeded more effectively with respect to the PA-6 single fibers. It has been shown that the Weibull's model is more correct for describing the statistical distributions of the mechanical properties of the high-strength PA-6 fibers than the Gaussian one. It has been shown that the data scatter for some of the mechanical properties (E_2, ε_b and $\varepsilon_{b\text{-}2}$), including those estimated, for the first time, by differentiating the stress-strain curves (E_2 and $\varepsilon_{b\text{-}2}$), is substantially smaller for the multifilament with respect to that for the single fibers due to the substantially larger (by two orders of magnitude) number of the fractured single fibers per test in the multifilament samples as compared to the single fibers, making the results received for the former more proper statistically. Basing on the results received in this work and earlier [2, 9–11], we guess that it is necessary to use both the Weibull's and Gaussian models for the correct statistical analysis of the mechanical properties of high-strength materials of various natures, both fragile and ductile.

REFERENCES

1. **Marikhin V.A., Myasnikova L.P.**, Structural basis of high-strength high-modulus polymers, In: *Oriented Polymer Materials*, Ed. S. Fakirov, Chapter 2 (1996) 38–98, Huthig & Wepf Verlag-Zug, Heidelberg.

2. **Boiko Yu.M., Marikhin V.A., Myasnikova L.P., Moskalyuk O.A., Radovanova E.I.**, Weibull statistics of tensile strength distribution of gel-cast ultra-oriented film threads of ultra-high-molecular-weight polyethylene, Journal of Materials Sciences. 52 (3) (2017) 1727–1735.

3. **Callister W.D., Rethwisch D.G.**, Characteristics, Applications, and Processing of Polymers, In: *Materials Science and Engineering*, 10th ed., (2020) Chapter 15, 523–576, Wiley.

4. **Boiko Yu.M., Kovriga V.V.**, Relaxation behavior of polyethylene oriented by various techniques, International Journal of Polymeric Materials. 22 (1-4) (1993) 209–217.

5. **Thomopoulos N.T.**, Statistical Distributions: Applications and Parameter Estimates (2017) 189 p., Springer International Publishing AG.

6. **Zok F.W.**, On weakest link theory and Weibull statistics. Journal of the American Ceramic Society. 100 (4) (2017) 1265–1268.

7. **Tanaka F., Okabe T., Okuda H., Kinloch I.A., Young R.J.**, Factors controlling the strength of carbon fiber in tension, Composites A. 57 (February) (2014) 88–94.

8. **Baikova L.G., Pesina T.I., Kireenko M.F., Tikhonova L.V., Kurkjian C.R.**, Strength of optical silica fibers measured in liquid nitrogen, Technical Physics. 60 (6) (2015) 869–872.

9. **Boiko Yu.M., Marikhin V.A., Moskalyuk O.A., Myasnikova L.P., Tsobkallo E.S.**, Statistical analysis of the tensile strength of oriented polyamide-6 fibers, Technical Physics Letters. 45 (4) (2019) 404–406.

10. **Boiko Yu.M., Marikhin V.A., Moskalyuk O.A., Myasnikova L.P., Tsobkallo E.S.**, Laws of statistical distribution of the mechanical properties of oriented polyamide-6 fibers, Technical Physics Letters. 45 (7) (2019) 707–710.

11. **Boiko Yu.M., Marikhin V.A., Myasnikova L.P., Radovanova E.I.**, Statistical viscoelastic and fracture mechanical properties of gel-cast ultra-oriented high-strength film threads of ultra-high-molecular-weight polyethylene, Colloid and Polymer Sciences. 296 (10) (2018) 1651–1656.

12. **Boiko Yu.M., Kovriga V.V.**, Deformation properties of self-reinforced polyethylene and their generalized description, Mechanics of Composite Materials. 27 (4) (1991) 392–397.

THE AUTHORS

BOIKO Yuri M.
yuri.boiko@mail.ioffe.ru
ORCID: 0000-0003-3031-5137

MARIKHIN Vyacheslav A.
v.marikhin@mail.ioffe.ru
ORCID: 0000-0001-7088-5914

MYASNIKOVA Liubov' P.
liu2000@mail.ru
ORCID: 0000-0003-0648-5056

Received 20.10.2022. Approved after reviewing 15.11.2022. Accepted 15.11.2022.